agriculture

MDPI

Article

Performance Analysis and Selection of Chinese Solar Greenhouses in Xinjiang Desert Area

Xiao Wu [1,†], Hong Li [1,†], Siyu Sang [1], Anhui He [1], Yimei Re [1] and Hongjun Xu [1,2,*]

1 College of Horticulture, Xinjiang Agricultural University, Urumqi 830052, China
2 Center for Postdoctoral Studies of Xinjiang Agricultural University, Urumqi 830052, China
* Correspondence: xhj@xjau.edu.cn; Tel.: +86-13609973416
† These authors contributed equally to this work.

Abstract: This study aims to provide information and theoretical support for the development planning of facility agriculture in desert areas. Using sensor monitoring, USB cable, and computer connection record, we measured the temperature, humidity, and heat transfer distribution of ordinary brick wall greenhouse (G1), composite wall greenhouse (G2), and assembled solar greenhouse (G3) in the Aksu desert area of Xinjiang. The results showed that G3 had the highest average temperature among the three types of greenhouses in the cold season; no difference was detected between G1 and G2 in the night temperature, while G3 has the characteristics of fast heating and cooling. On a sunny day, the heating rate of G1, G2, and G3 is 3.62, 4.4, and 4.77 °C/h, respectively. The cooling rate for G1 is 2.66 °C/h; 2.96 °C/h for G2; and 3.93 °C/h for G3. The heating rate for each greenhouse is nearly identical when it is cloudy outside, and the cooling rate of G1, G2, and G3 is 2.71, 4.2, and 4.34 °C/h, respectively. Moreover, the G3 north wall's thermal insulation performance has clear advantages. Its wall surface can reach a temperature of 59.1 °C (G1 is 42.7 °C and G2 is 41.6 °C). This study showed that G3 possesses the virtues of effective thermal insulation; the rear wall has a small footprint and preserves the arable land; it also achieves the necessary environmental conditions for crop growth without the use of auxiliary heating.

Keywords: solar greenhouse; north wall; light and thermal environment; assembled solar greenhouse

check for updates

Citation: Wu, X.; Li, H.; Sang, S.; He, A.; Re, Y.; Xu, H. Performance Analysis and Selection of Chinese Solar Greenhouses in Xinjiang Desert Area. *Agriculture* **2023**, *13*, 306. https://doi.org/10.3390/agriculture13020306

Academic Editor: Massimo Cecchini

Received: 20 December 2022
Revised: 17 January 2023
Accepted: 20 January 2023
Published: 27 January 2023

1. Introduction

About 13.36% of the earth's surface is composed of deserts, including the Gobi Desert [1–4]. Northwest China is a large region with a wealth of untapped resources in uncultivated soil. Xingjiang belongs to the temperate continental climate, the temperature difference between day and night is large, but the sunshine time is sufficient, with little precipitation, and dry climate. Despite constituting 1/6th of China's total land area, it severely lacks resources for land cultivation (Figure 1). Xinjiang has a per capita cultivated land area of just 0.2 hm^2 [5]. This continuously encourages the expansion of facility agriculture in Xinjiang to uncultivated land, such as the Gobi, saline-alkali, and desert land. One of the critical solutions to the lack of rigidity of cultivated land resources in our area has been to find ways to enhance the usage of non-cultivated land resources. This has also become an essential strategy for promoting the sustainable growth of facility agriculture in Xinjiang [6].

Chinese solar greenhouse (CSG) is used to grow plants in the winter without any ancillary heating, as it is cheap and an efficient way to protect crops from the elements. Covered and uncovered thermal blankets are used to lessen the heat released to the environment. A south roof is made of plastic, glass, or other material. The north wall stores heat during the day and releases it at night (Figure 2) to raise the temperature and avoid low temperatures. In China, there are several types of greenhouses. CSGs have created new opportunities for the horticulture business [7]. Rapid urbanization has improved the quality of life, socioeconomic development, and other areas. In addition, it directly disrupts the original pattern of the cultivated land, and the cultivated land area is occupied [8]. Due to the factors above, the CSG construction area has grown annually. Moreover, CSGs have specific production and operational advantages depending on the local climate and environment, in addition to a wide range of structural variations depending on the locale. The wall structure and building materials of CSGs are varied, with noticeable differences [9]. This has a considerable impact on the light and thermal environment of the CSG. In order to further improve the thermal performance of the greenhouse and tap the potential of the north wall, Liu et al. analyzed four passive heat storage north walls based on CFD. The results show that the heat storage capacity of the north wall is affected by the surface structure and is directly related to the thermal environment of the solar greenhouse [10]. In addition to the optimization of wall materials, a lot of research has been carried out in terms of ridge position ratio, rear roof projection width, north wall height and thickness [11–13]. It is found that the thermal environment of solar greenhouse is closely related to these factors. Therefore, studying the light and temperature performance of various CSG types is crucial, similar to choosing the most cost-effective CSGs that fit the local production demands for promotion and demonstration to increase the planting efficiency of the greenhouses across diverse locations.

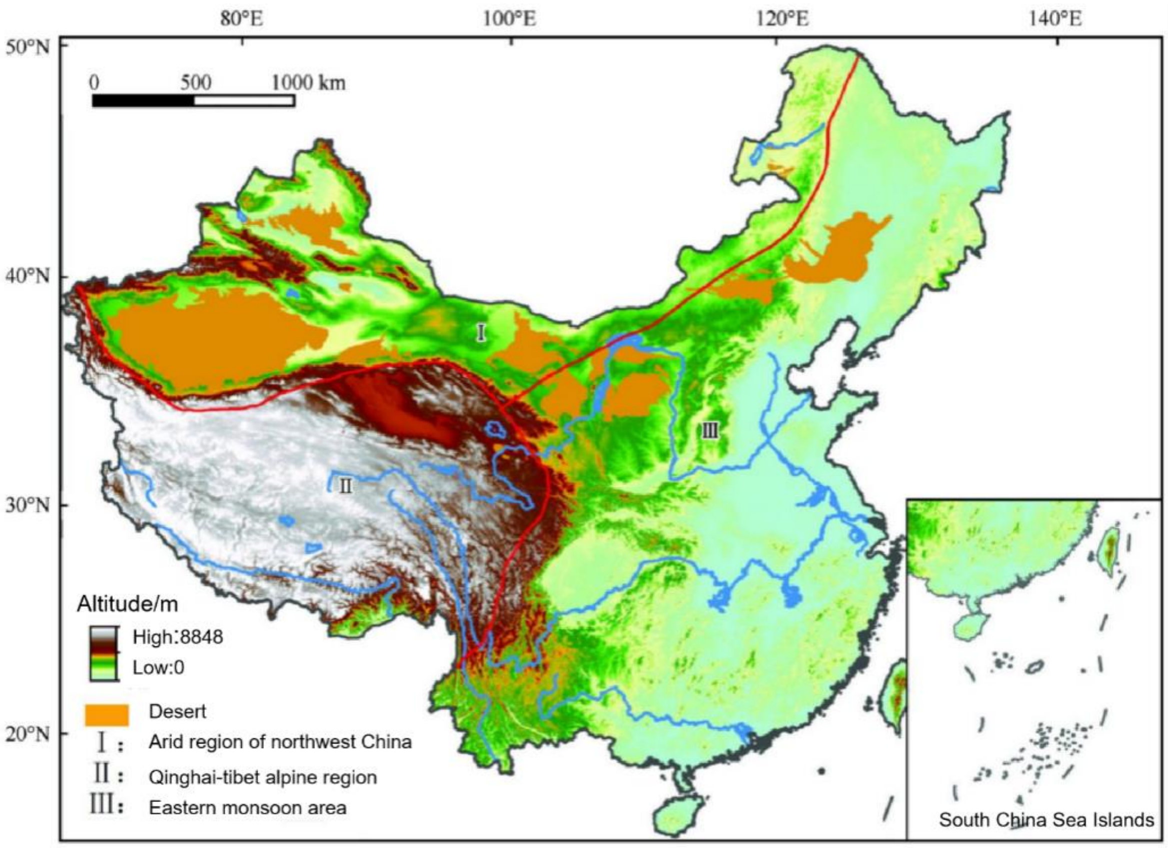

Figure 1. Schematic of the desert and sandy land areas in China.

Since they can provide a suitable climate for the growth of crops, which is unique in agricultural development, CSGs are ideal for development and exploitation in non-arable places. A poor land usage rate has been recorded, and the cultivated land has suffered irreparable harm. In uncultivated soil with delicate biological conditions, the conventional north wall is inapplicable. The internal ambient microclimate of various greenhouses has been thoroughly analyzed and compared to previous studies, with a primary emphasis on the wall materials of CSGs and their heat preservation capabilities [14–21]. Although the performance of the wall in terms of heat storage and preservation is partial and reflected from various angles, the wall's ability to transfer heat under complex environmental conditions makes it impossible to evaluate the environment in a greenhouse solely based on the wall's performance. This study measures the Xinjiang desert region's three typical CSG structural properties and environmental performance. The CSG was summarized by field research and parameter comparison; vegetable production during the winter can be accomplished without supplemental heating. It offers a theoretical framework for choosing an appropriate CSG for the Xinjiang desert region.

Figure 2. Internal views of CSG.

2. Material and Methods

2.1. Overview of the CSGs

G1 is a south-facing brick construction, with a north-south span of 9 m, an east and west length of 75 m each, a height of 4 m, a north wall height of 2.5 m, and a thickness of 60 cm. G2 is a south-facing construction. The north-south span is 10 m, the east-west span is 72 m, the ridge height is 5.2 m, and the height for the north wall is 4 m. Brick and benzene board constitute the north wall, which is 50 cm thick (20 cm bricks, 10 cm benzene boards, and 20 cm bricks). G3 is made up of galvanized steel pipes and polyester wadding, and is south-facing; the north-south span is 12 m, the east-west span is 72 m, its height is 5.2 m, and its north wall's height is 4 m (Figure 3).

G1 G2 G3

Figure 3. Three types of CSGs for test.

During testing, the transmittance of the three greenhouses, including the plastic film covering material, seemed consistent. *Solanaceous* vegetables are the main crop cultivated in the greenhouse using drip irrigation. On sunny days, the thermal blanket is rolled up at 10:00 a.m. and rolled down at 19:30. On cloudy days, it is rolled up at 11:00 a.m. and rolled down at 17:30 to reduce heat loss at night. Throughout the whole manufacturing process, there is no auxiliary heating or ventilation in the greenhouse.

2.2. CSG Environment Monitoring

2.2.1. Test Contents

From January–March 2022, the greenhouse underwent environmental monitoring. The main environmental variables, such as soil and wall temperatures, humidity, solar radiation, and heat transfer, were measured through the envelope. The data were recorded at 10-min intervals at all measuring points.

2.2.2. Test Equipment

The PDE-RI temperature data recorder (Harbin Wage Electronic Technology Co., Ltd., Heilongjiang, China, temperature measuring range: 20–60 °C, accuracy: 0.5 °C, resolution: 0.1 °C) was used to record the data on air temperature, humidity, and soil temperature. The PDE-RI environmental data recorder (measurement range: 0–2000 W/m^2, accuracy 3%, resolution 1 W/m^2) was used to capture the solar radiation. Use TNRL-20 soil heat flux sensor (sensitivity coefficient: 23.26 W/m^2) to measure the heat flow through the enclosure construction (The Jinzhou Tiannuo Environmental Instrument Co., Ltd., Liaoning, China) [22].

2.2.3. Layout of Measuring Points

The temperature and humidity measurement points are located in the length direction 1/2 and span direction 1/2 of the indoor greenhouse (shown in Figure 4), with the height of 1.5 m, 1 m, and 0 m; the outdoor distance from the front of the greenhouse is 2 m and the height is 1.5 m. The measuring points of soil temperature are located in 1/2 of the length direction and 1/2 of the span direction of the indoor greenhouse. The measuring depth is 50 cm, and the distance between each measuring point is 10 cm, the measuring points were set in the vertical direction, 0, 10, 20, 30, 40, and 50 cm away from the soil surface. The temperature measurement point of the wall is located at 1/2 of the north wall, with a height of 1.5 m.

2.3. Statistical Analyses

An analysis of the heating and cooling rate is a crucial starting point for assessing the thermal environment of north walls. The following are the steps involved in calculating the heating and cooling rates [23]:

$$k_{Tup} = \frac{\left|T_{start(\mathrm{up})} - T_{end(\mathrm{up})}\right|}{\Delta_{tup}} \tag{1}$$

$$k_{Tdown} = \frac{\left|T_{start(\mathrm{down})} - T_{end(\mathrm{down})}\right|}{\Delta_{tdown}} \tag{2}$$

where k_{Tup} is the daily heating rate of the greenhouse, °C/h; k_{Tdown} is the cooling rate of the greenhouse, °C/h; $T_{start(\mathrm{up})}$ and $T_{end(\mathrm{up})}$ are the starting and ending temperatures, °C; $T_{start(\mathrm{down})}$ and $T_{end(\mathrm{down})}$ are the initial temperature and end temperature of the cooling stage, °C; Δ_{tup} is the heating time, h; Δ_{tdown} is the cooling time, h.

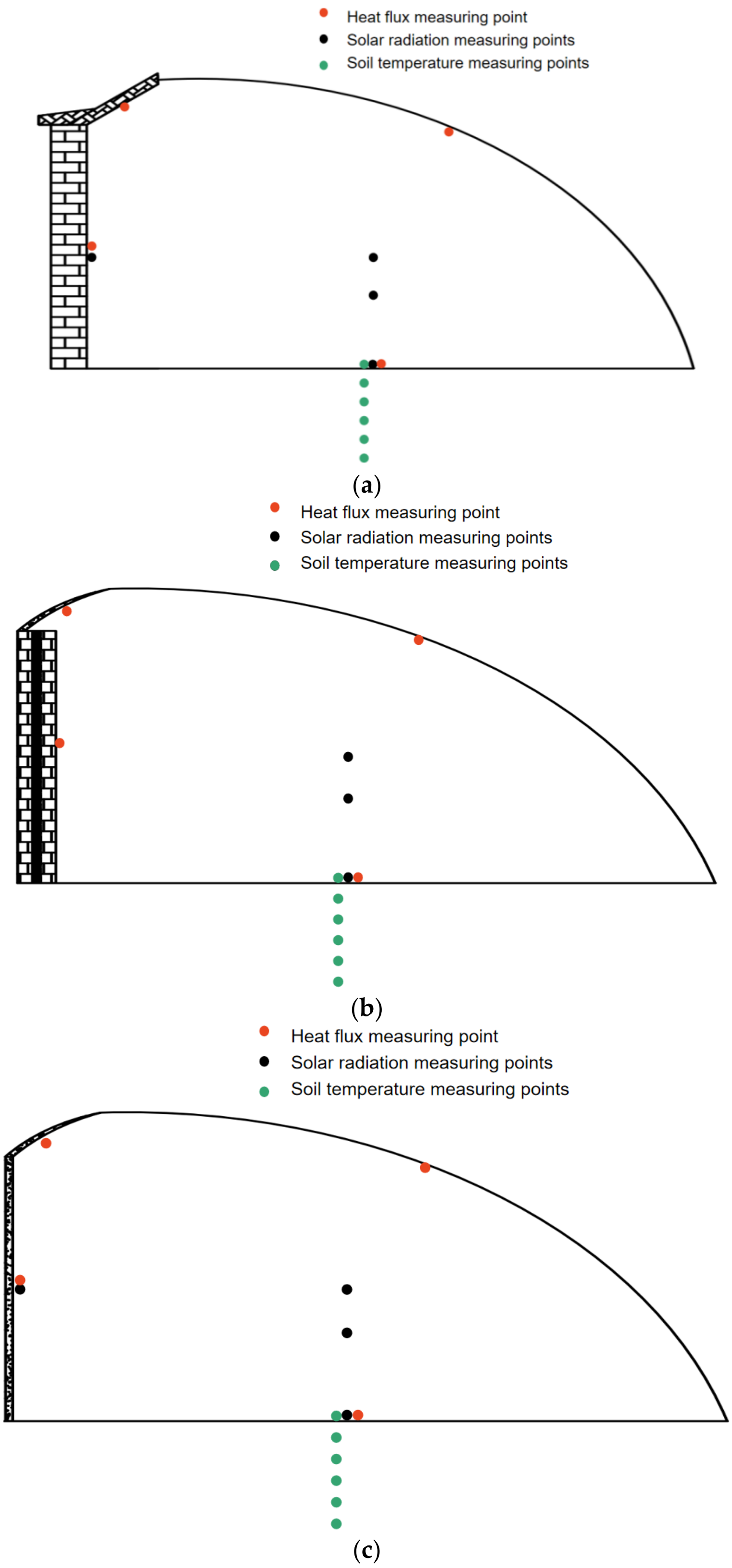

Figure 4. Distribution of environmental testing points in CSG. (**a**) Distribution of environmental testing points in G1. (**b**) Distribution of environmental testing points in G2. (**c**) Distribution of environmental testing points in G3.

3. Results and Analysis

Three greenhouses were tested between January and March on typical sunny days (28 January, 20 February and 31 March 2022) to examine the internal environmental changes.

3.1. CSG Environment Change Analysis

3.1.1. Variation in Solar Radiation

As shown in Figure 5, outdoor solar radiation is greater than indoor. The variation follows a consistent pattern. As the month progresses, solar radiation increases significantly.

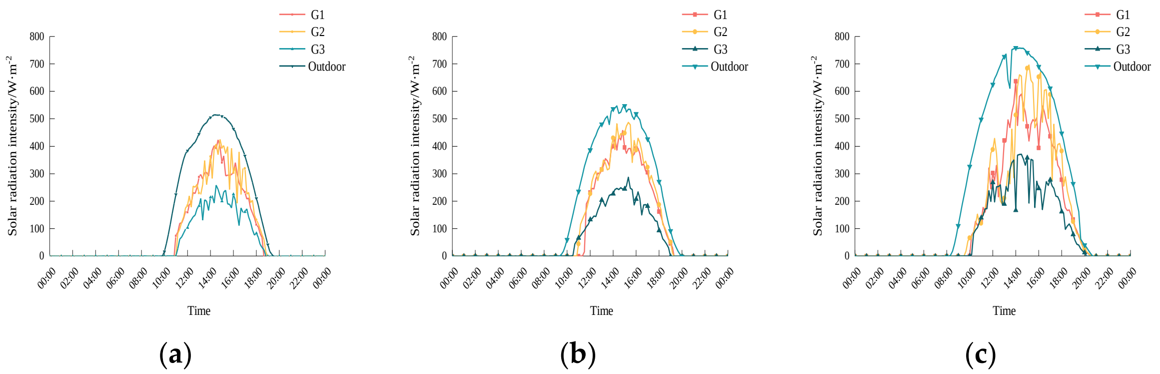

Figure 5. Variation in solar irradiation on typically bright days between January and March. (**a**) 28 January 2022. (**b**) 20 February 2022. (**c**) 31 March 2022.

We screened out the typical sunny days each month (Figure 5). On January 28, the daytime average solar radiation of G1 was an average of 242 W/m^2, G2 was 247.1 W/m^2, and G3 was 146.4 W/m^2; on February 20, it was 281.8 W/m^2 for G1, 290 W/m^2 for G2, and 159.2 W/m^2 for G3; On March 31, it was 308.3, 316.8 W/m^2, and 204.7 W/m^2 for G1, G2, and G3, respectively. According to the results, G3 received the least amount of solar energy, and G1 and G2 barely differed.

3.1.2. Variation in Temperature

Temperature is a significant environmental component influencing plant productivity and distribution. It is a crucial index to evaluate the thermal environment. Temperature fluctuations of each greenhouse, indoors and outdoors under typical sunny conditions, are shown in Figure 6. The G3 greenhouse had a better insulation effect compared to the other two greenhouses because of its minor temperature fluctuations and sluggish response to temperature changes. Thus, G3 always had a warmer daytime temperature than G1 and G2.

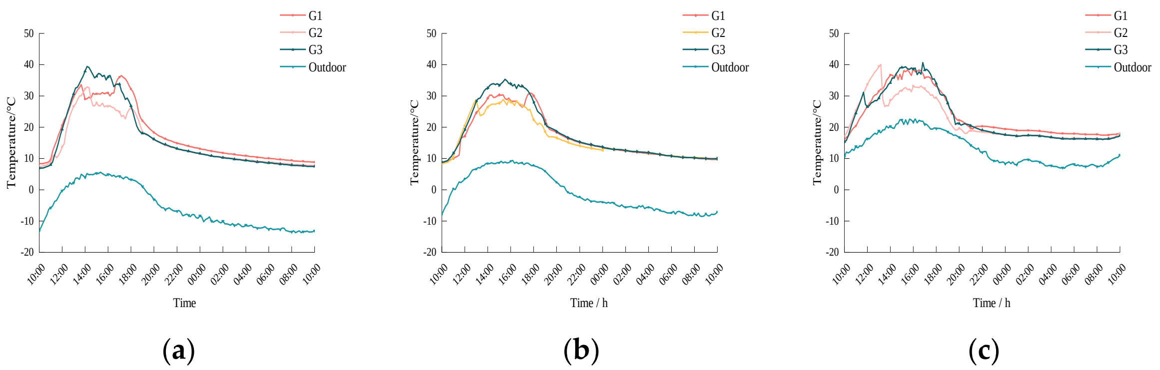

Figure 6. Temperature variation of CSGs on typical sunny days from January to March. (**a**) 28 January 2022. (**b**) 20 February 2022. (**c**) 31 March 2022.

On January 28, the daytime temperatures in the greenhouses were as follows: 25.7 °C in G1, 21.7 °C in G2, and 25.9 °C in G3. On February 20, G1, G2, and G3 had an average daytime temperature of 27.1 °C, 25.1 °C, and 25.2 °C, respectively. On March 31, the temperatures were 30.9 °C, 29.3 °C, and 31.5 °C in G1, G2, and G3, respectively. The minimum temperature at night is one key indicator while evaluating the benefits of the greenhouse environment. On January 28, the extreme minimum temperature in G1 was 8.8 °C, 7.7 °C in G2, and 7.5 °C in G3. On February 20, the lowest temperatures recorded were 10.7 °C in G1, 9.9 °C in G2, and 9.9 °C in G3, while these were 17.5 °C in G1, 16.3 °C in G2, and 16.1 °C in G3 on 31 March 2022.

Since the essence of convective heat transfer is the difference in air density, when the temperature difference is slight, air heat transfer occurs more quickly and efficiently. An uneven temperature distribution hinders plant growth in a CSG. On sunny days, the temperature difference between the measuring points of 0–1 m was as follows: G1 0.779 °C, G2 0.685 °C, and G3 1.076 °C, while on cloudy days, G1 was 0.833 °C, G2 was 0.808 °C, and G3 was 1.039 °C. Thus, although G3 has clear temperature advantages, its thermal stability is less than that of G1 and G2.

3.1.3. Variation in Humidity

The humidity of the indoor air is a crucial meteorological factor for assessing the microclimate in greenhouses. Crop production benefits from an appropriate humidity level are also evaluated.

Figure 7 shows how indoor relative humidity varies on sunny days throughout the year. The three experimental CSGs' average relative humidity was funnel-shaped during the day and stayed above 85% for most of the time. When the thermal blanket was uncovered, the humidity declined rapidly with rising temperature. Conversely, the humidity rose progressively at night after the blanket was covered due to the drop in temperature. G3 had marginally greater humidity than G1 and G2. Because of less solar radiation, the humidity also rose significantly on cloudy days. When the ventilation opening closes, plant respiration releases water, resulting in a drop in temperature and an increase in humidity. Consequently, the dry north wall absorbs the internal water. Thus, dehumidification is essential during the production process in G3 to prevent disease outbreaks on the plant caused by high humidity.

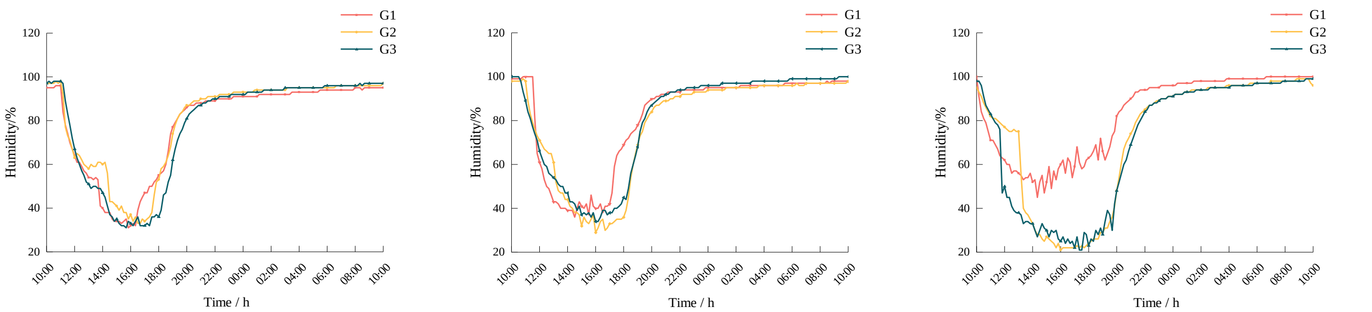

(**a**) (**b**) (**c**)

Figure 7. Humidity variation of CSGs on typical sunny days from January to March. (**a**) 28 January 2022. (**b**) 20 February 2022. (**c**) 31 March 2022.

3.2. CSG Performance Analysis

Because the temperature rate, wall surface temperature, and soil thermal performance have similar trends across months, we selected only typical sunny days (20 February 2022) and cloudy days (18 February 2022) in the same month for examination in the follow-up study.

3.2.1. Temperature Variation Rate in CSGs

The temperatures of the three CSGs peaked at different times. The maximum temperature of G1 on sunny days was 33.7 °C at 17:50. At 15:00, G2 achieved its highest temperature of 35.7 °C, while at 15:10, G3 reached its highest temperature of 39.3 °C. G1 reached its maximal temperature of 29.4 °C at 15:00 on cloudy days, while G2 had its highest temperature of 29.9 °C at 15:30, and G3 reached its maximum temperature at 16:10. The heating rates of the three CSGs were determined to be 3.62, 4.4, and 4.77 °C/h for G1, G2, and G3, respectively. According to the statistics, G3 heats the fastest once the heat preservation is turned off, followed by G2 and G1. The rate of heating in each greenhouse hardly varies on cloudy days. The temperature gradually started to drop when the peak interior temperature was reached. Under normal sunny conditions, G1 cooled down at a rate of 2.66 °C/h, G3 at 3.93 °C/h, and G2 at 2.96 °C/h. On cloudy days, G1 cooled at a rate of 2.71 °C/h, G2 at 4.2 °C/h, and G3 at 4.34 °C/h. The quickest cooling rate was observed in G3.

3.2.2. Temperature Variation in the Wall Surface of CSG

The north wall absorbs and stores the extra heat produced during the day, and at night, when the temperature drops sufficiently, the north wall transmits the heat accumulated to the greenhouse through a heat exchange. The wall heat flux variations of each greenhouse in the image can be noticed. The G3's wall heat flux change is unique in that it scarcely releases heat into the space at night (Figure 8). Since G3 does not have a north wall to store heat, there is no daytime heat buildup. Around 16:00 in cloudy weather, a tiny amount of heat accumulated by thermal radiation is released due to the greenhouse's high temperature.

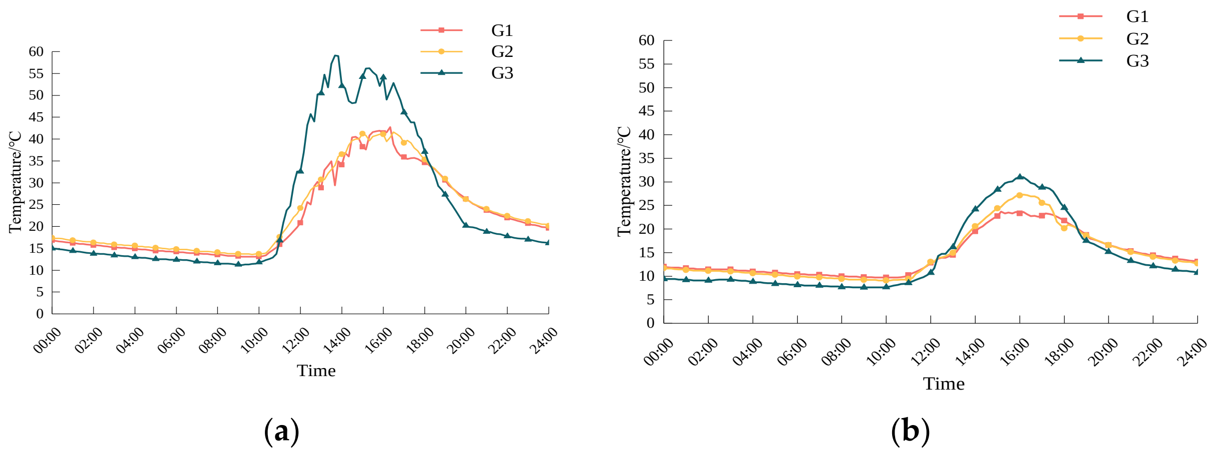

Figure 8. Wall surface temperature variation of CSGs under typical weather. (**a**) Sunny day (20 February 2022). (**b**) Cloudy day (18 February 2022).

Figure 8 illustrates how the north wall's surface temperature variation is steadier on gloomy days than on sunny days. The assembled CSGs' wall temperature is the highest, with a rapid heating rate. Under cloudy conditions, the maximum temperature of the G1, G2, and G3 wall surfaces was 23.7, 27.3, and 31 °C, respectively. Compared to other greenhouses, the G3 daytime wall's surface temperature was significantly higher in sunny conditions, reaching 59.1 °C (G1 was 42.7 °C and G2 was 41.6 °C). One of the factors contributing to G3's outstanding heat transfer efficiency was that after the heat preservation blanket was covered, the wall temperature dropped quickly, and the wall surface temperature in the three CSGs stayed the lowest at night. Since the greenhouse lacks a north wall that serves as a significant heat storage structure, the wall primarily receives heat by conduction when the insulation blanket is uncovered. The energy transfer inside the greenhouse has three directions, heat loss to the outside through the wall, heat storage inside the wall, and convection through the air indoors. In this study, the north walls of G1 and G2 have heat storage capabilities, and some heat is stored for use at night. Since G3 wall material is unique, it has an excellent thermal insulation effect, such that the heat loss is very less through the wall to the exterior. Hence, the G3 wall surface heating rate is quick and the temperature is high, maintaining the best thermal environment in G3 regardless of the weather.

Among the three test CSGs, heating and cooling effectuate most quickly in G3. The greenhouse heat is mostly transferred through conduction, convection, and radiation, with radiation heat transfer constituting the majority of the total heat transmission. Since the north wall of G3 has no heat storage capacity, solar energy that enters indoors and progressively radiates to the wall is reflected mainly off the surfaces within the building, and then convectionally transferred to the interior air. G1 and G2 receive solar radiation on their north walls to store the heat. Part of the heat is conveyed to the interior air, while the other part is retained as heat in the wall, resulting in a slow heating and cooling process.

3.2.3. Different CSG Wall Thermal Performance Test

The extra heat in the CSG is absorbed and stored by the wall during the day. The heat exchange occurs between the wall at night. Each wall heat flux change is illustrated in the image (Figure 9). The G3's wall heat flux change stands out, and its north wall scarcely releases heat indoors at night. Around 16:00 on a cloudy day, due to the high temperature of the greenhouse, a small amount of heat accumulated by thermal radiation is released.

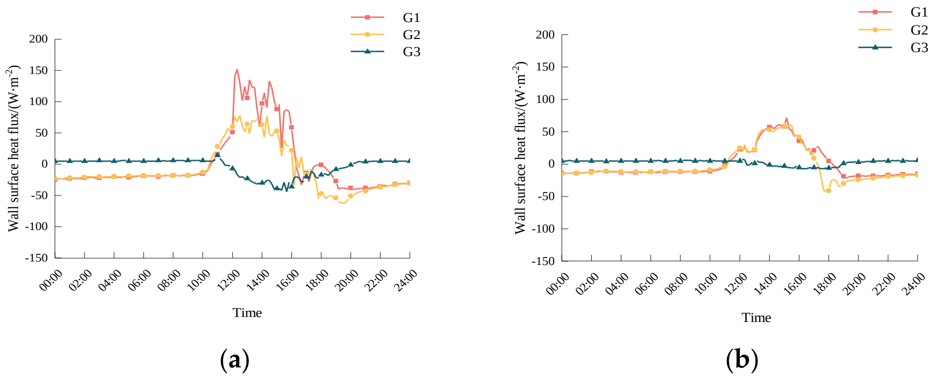

Figure 9. Changes in heat flux on the wall surface of CSGs under typical weather. (**a**) Sunny day (20 February 2022). (**b**) Cloudy day (18 February 2022).

3.2.4. Heat Storage Performance of Soil in Different CSGs

In a greenhouse without heating, the soil serves as the only heat source and heat storage medium. In order to understand the thermal environment of G3, it is essential to analyze the soil temperature distribution, fluctuation law, and heat storage and release properties of the soil.

Figure 10 shows that solar radiation penetrates the greenhouse and irradiates the soil surface after the thermal blanket is uncovered. Based on the soil temperature, it is evident that the soil starts to absorb and store heat at this point. G2 and G3 conserved more heat than G1 soil on cloudy days. G2 stored the most heat during daytime on sunny days, while G1 and G3 presented similar values. Although the heat received by the greenhouse soil varies markedly during the day, the heat that the soil supplies to the greenhouse at night is almost constant and does not show any visible peaks or fluctuations. G3 performs better in thermal insulation and has a higher temperature at night. Since there is less heat demand in G1 and G2 than in G3, there is less heat loss in the soil. The three CSGs had an average daily heat flux of 40.29 W/m^2, 65.89 W/m^2, and 39.72 W/m^2 on sunny days and an average heat flux of -16.85 W/m^2, -17.04 W/m^2, and -20.59 W/m^2 at night, respectively. The average heat flux during the day and night on cloudy days was 32.56 W/m^2, 61.19 W/m^2, and 51.92 W/m^2 and -20.4 W/m^2, -18.49 W/m^2, and -21.2 W/m^2, respectively. As the soil can store and release a large amount of energy at a higher temperature when it is cooler, the soil heat release of G3 is the highest at night. Thus, it can be observed that G3 soil has more significant buffering properties and is better at controlling the greenhouse's thermal environment than the other two types.

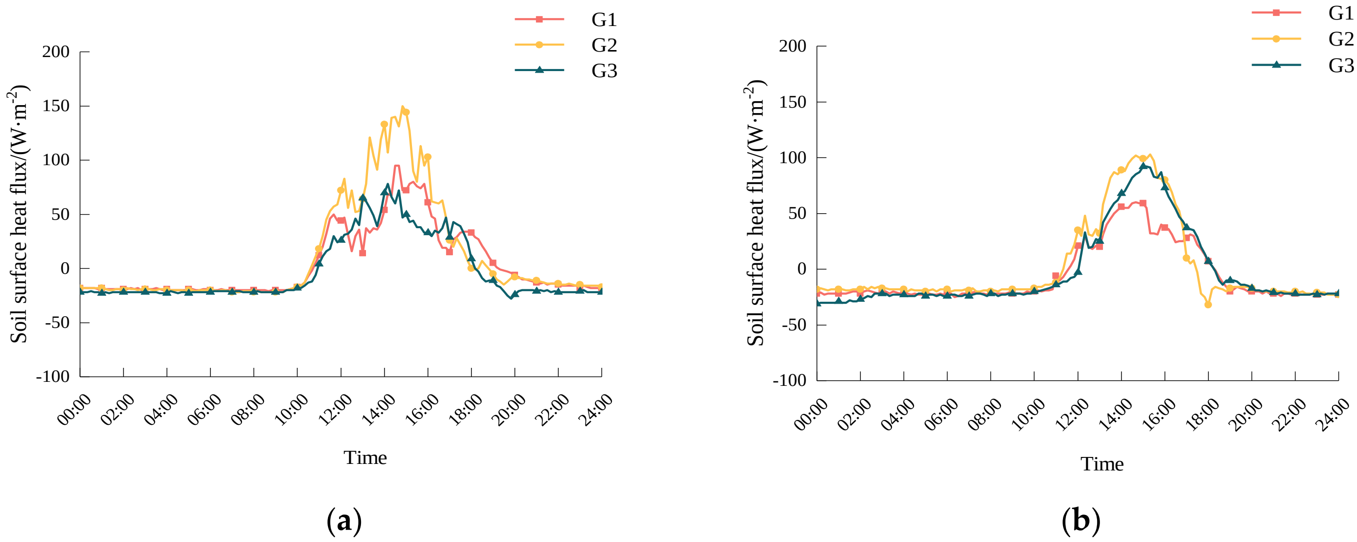

Figure 10. Variation of soil surface heat flux in typical weather in CSGs. (**a**) Sunny day (20 February 2022). (**b**) Cloudy day (18 February 2022).

3.2.5. Determination of Soil Thermal Storage Layer

The ability to store and release soil heat is essential in CSGs. When the temperature of the soil depth varies greatly, convective heat transfer between soil and air inside the greenhouse becomes stronger, maintaining the stability of the temperature at night. Based on the temperature differential measurement, it could be deduced that there is a gain in the thickness of the soil's heat storage layer. The more heat the soil stores during the day or releases at night, the greater the temperature difference between the soil at various depths.

The thickness of the soil heat storage layer in each greenhouse was measured to about 20 cm in sunny weather (Table 1), while in cloudy weather, the thickness of the soil heat storage layer in the G3 reached 40 cm. This created ideal conditions for heat storage during the day and heat release at night in the G3, rendering another reason why, despite the cloudy weather and low outdoor temperature, the internal temperature of the G3 is high and consistent. Nonetheless, it must release soil heat to compensate for some of the greenhouse system's heat loss at night.

Table 1. Thickness of heat storage layer of soil in each greenhouse determined by temperature difference methods.

Types of CSG	Thermal Blanket	Soil Depth on a Typical Sunny Day						Soil Depth on a Typical Cloudy Day					
		0.5 m	0.4 m	0.3 m	0.2 m	0.1 m	0 m	0.5 m	0.4 m	0.3 m	0.2 m	0.1 m	0 m
G1	Uncovered	17.6	17.6	17.4	16.5	15.4	12.6	17.4	17.2	16.5	15.0	13.6	10.9
	Covered	17.5	17.5	17.7	18.3	19.2	19.0	17.1	16.9	16.8	17.2	18.3	18.7
G2	Uncovered	17.8	18.0	18.1	17.9	17.0	15.0	17.0	16.9	16.5	15.7	14.1	10.7
	Covered	17.7	17.9	18.1	18.6	19.2	18.7	16.7	16.5	16.7	17.7	17.7	17.5
G3	Uncovered	18.0	18.3	18.4	18.2	16.9	14.7	15.7	14.6	13.9	12.8	12.0	11.4
	Covered	17.9	18.2	18.7	19.9	21.5	21.2	16.1	15.9	15.6	16.4	18.5	19.5

3.2.6. Calculation of Soil Heat Transfer

The heat transfer process in the soil of the CSG involves conduction, convection, evaporation, and condensation [24]. The changes in the data indicate that G3 soil releases maximal heat, and the whole process is stable (Table 2). The cumulative heat release of G3 is 1.13 MJ on sunny days (G1 is 1.33 MJ, G2 is 1.15 MJ) and 1.33 MJ on cloudy days (G1 is 1.37 MJ, G2 is 1.41 MJ). Irrespective of the weather, the soil's daily cumulative heat loss is greater than the daily cumulative heat storage. This phenomenon could be attributed to heat accumulation in the soil on sunny days. The accumulated heat is released when it is cold at night to warm the greenhouse's thermal environment.

Table 2. Soil heat storage and release performance parameters.

Weather Conditions	Types of CSG	Daily Accumulation Heat/(MJ/m^2)	Heat Storage Duration/h	Max Heat Storage Flow/(W/m^2)	Daily Accumulated Heat Release/(MJ/m^2)	Heat Release Duration/h	Max Heat Release Flow/(W/m^2)
Sunny day (20 February 2022)	G1	1.32	6	103	1.33	18	27
	G2	1.73	7.5	186	1.15	16.5	34
	G3	1.59	7	90	1.13	17	24
Cloudy day (18 February 2022)	G1	0.78	6.7	60	1.37	17.3	25
	G2	1.32	6	103	1.41	18	32
	G3	1.15	6.2	92	1.33	17.8	31

3.2.7. Variation in Heat Flux of North Roof

The heat supplied by the soil to the shed at night was determined to be relatively constant, with no evident peak and only a slight fluctuation, after observing the variation in the soil heat flux (Figure 11). G1 releases the least heat, whereas G2 and G3 release maximum heat. The temperature rises gradually when the thermal blanket is uncovered. The north roof's heat loss increases progressively. The average temperature difference, the area of heat transfer, and the heat transfer coefficient affect how much heat is transferred. When the thermal blanket is covered, the indoor temperatures of G2 and G3 rise rapidly, and the corresponding difference between the indoor and outdoor temperatures is the highest. At 14:00, the north roof's heat release dropped progressively after each CSG. A portion of the heat entered the room through the north roof and continued until 19:30, as the heat flux density of the G2 and G3 turned negative. G1 released heat over this period, as observed by the structure's almost positive heat flux density. Thus, it is evident that G1's north roof solely loses heat, whereas G2 and G3's internal heat is obtained partially through the north roof. Notably, the direction of heat transfer from the north roof changes over time. The direction of heat transfer for the north roofs of G2 and G3 dramatically alters when the greenhouse achieves its highest temperature. Because the north roof of the G2 and G3 has a weak thermal insulation performance, it has little capacity to store heat and some scattered light energy that absorbs heat. When the greenhouse's interior temperature is maximal, heat radiates from the north roof and is brought back inside. The phenomenon on a cloudy day is similar to a sunny day. The north roof heat is released to the outside since the thermal blanket has been covered. G3 dissipates the maximal heat, followed by G2, while G1 dissipates the least heat. The north roof of G1 was still losing heat to the exterior when the thermal blanket was uncovered in the morning after solar radiation had entered the indoors. The amount of heating loss peaked when the interior temperature was the highest. The north roof of both G2 and G3 experience steady heat entry while the inside temperature rises steadily. G2 stores more heat during the day through its north roof compared to G3, as observed by the changing trend. However, G2 is also most susceptible to outside heat loss at night.

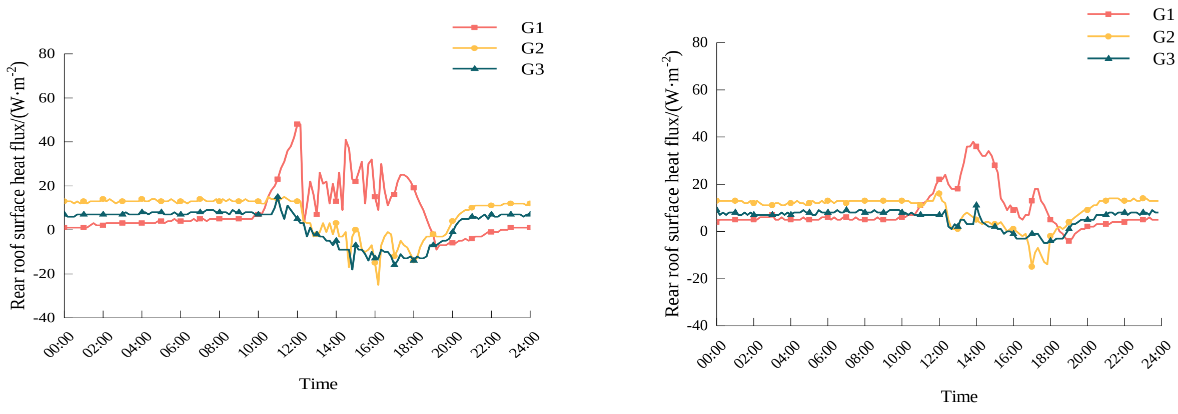

(**a**) (**b**)

Figure 11. Heat flow change in the north roof of CSGs under typical weather. (**a**) Sunny day (20 February 2022). (**b**) Cloudy day (18 February 2022).

Solar radiation is the only source of heat in a solar greenhouse. Part of the heat obtained in the greenhouse is stored in the walls or soil, while the other part is lost to the outside through the front roof, back roof, and walls. It has been discovered through the analysis of internal environmental data from various types of solar greenhouses that the solar radiation obtained by the three tested greenhouses during the day can satisfy the needs for temperature and light during the growing process of crops without the use of auxiliary heating and ventilation. Even though G3 receives less solar radiation, its performance in terms of temperature is superior because of the particular wall material's excellent thermal insulation performance. In addition, brick, which is a member of the multi-empty media, is the primary component of the walls of buildings G1 and G2. It has a certain ability to absorb water from the air in relatively dry environments, which also has a certain effect on the humidity in the greenhouse. Temperature affects humidity, while humidity changes with temperature. One of the reasons why the internal temperature of G3 is a little lower at night than that of the other two greenhouses is because higher humidity will cause solar greenhouses to cool down.

4. Discussion

The major body for storing and releasing heat in a CSG is its wall, which is one of the most often utilized horticultural facilities in agricultural output. Currently, increasing the thickness of a wall [25], adding more thermal insulation to the covering, and adding more thermal insulation materials [26], are the most popular techniques to increase the wall's ability to store and release heat, but their effectiveness is limited. The air temperature, humidity, soil temperature, solar irradiance, and greenhouse envelope heat flux, along with the actual production requirements, of three different wall structures of CSGs in the desert region of Aksu, Xinjiang, were used as research parameters. The findings demonstrated that the assembled CSG minimizes the area of the wall and satisfies the fundamental requirements for crop development without supplemental heating. The greenhouse's thermal climate could be established and maintained due to the wall's structure and materials, making the greenhouse design workable. According to comparison analysis, the assembled CSG exhibits quick heating and cooling, which is compatible with the findings of Peng et al. [27], and the environment in the G3 is in a high humidity state. Dehumidification must be stressed in the following products to prevent the spread of illnesses. The enclosure structure in the greenhouse can store and release heat in different ways. In the subsequent studies, tracking, collecting the thermal performance metrics in real-time, and computing the heat storage and release precisely need to be enhanced.

5. Conclusions

This study examined the thermal environment and microclimate variations in various greenhouses. The most popular three types of CSGs in the Aksu area of Xinjiang are compared in this study with respect to the internal environments of the assembled CSG, composite wall CSG, and ordinary brick wall CSG. The following conclusions are drawn:

(1) Irrespective of sunny or cloudy, the interior daytime temperature of the assembled CSG is significantly greater than that of the other two greenhouses. The difference in overnight temperatures among the three CSGs is small. Even when some solar radiation is reflected on cloudy days, the assembled CSG can maintain a high-temperature environment. Additionally, the assembled CSG has poor thermal stability and exhibits the traits of fast heating and cooling. However, the wide temperature range of the greenhouse is suitable for plant growth.

(2) In this study, the assembled CSG's wall surface temperature is significantly greater than that of the other two types of CSGs, and this difference has a marked impact on the greenhouse's air temperature.

(3) Due to the special wall materials used in the assembled CSG, it has been discovered that the indoor heat loss of the structure to the outside is very small. The soil with the thermal storage layer thicker than that of the other two types of greenhouses, provides the majority of the heat. In addition to realizing the effective use of light energy, this type of CSG also reduces construction cost and time, maximizes the CSG's capacity for thermal insulation. We know from the survey that the cost per square meter of research brick solar greenhouse is basically 490 CNY, composite wall greenhouse need is 360 CNY, and assembled solar greenhouse is 300 CNY. In conclusion, the assembled solar greenhouse has a positive marketing value.

Author Contributions: Conceptualization, A.H., S.S. and Y.R.; methodology, X.W., S.S. and H.X.; writing—original draft preparation, X.W., H.X. and H.L.; writing—review and editing, H.L. and H.X.; supervision, H.X. and H.L. All authors have read and agreed to the published version of th manuscript.

Funding: This research was funded by [the Natural Science Foundation of Xinjiang Uygur Autonomous Region] grant number [2021D01A83], he National Natural Science Foundation of China grant number [32260437] and the Natural Science Youth Project of the Autonomous Region University Scientific Research Program grant number [XJEDU2019Y017].

Institutional Review Board Statement: Not applicable.

Data Availability Statement: The data presented in this study are available in the article.

Conflicts of Interest: The authors declare no conflict of interest.

References

1. Zhang, G.; Shi, Y.; Liu, H.; Fei, Z.; Liu, X.; Wei, M.; Liu, F.; Wang, S. Heat transfer performance of an assembled multilayer wall in a Chinese solar greenhouse considering humidity. *J. Energy Storage* **2021**, *33*, 102046. [CrossRef]
2. Sternberg, T.; Rueff, H.; Middleton, N. Contraction of the Gobi desert, 2000–2012. *Remote Sens.* **2015**, *7*, 1346–1358. [CrossRef]
3. Cai, L.; Wang, H.; Liu, Y.; Fan, D.; Li, X. Is potential cultivated land expanding or shrinking in the dryland of China? Spatiotemporal evaluation based on remote sensing and SVM. *Land Use Policy* **2022**, *112*, 105871. [CrossRef]
4. Cui, Y.; Liu, J.; Xu, X.; Dong, J.; Li, N.; Fu, Y.; Lu, S.; Xia, H.; Si, B.; Xiao, X. Accelerating cities in an unsustainable landscape: Urban expansion and cropland occupation in China, 1990–2030. *Sustainability* **2019**, *11*, 2283. [CrossRef]
5. Wang, D.; Wu, S.; Zhang, S. Expansion of both cultivated and construction land in Xinjiang since the late 1980s. *Arid. Land Geogr.* **2017**, *40*, 188–196.
6. Xie, J.; Yu, J.; Chen, B.; Feng, Z.; Lyu, J.; Hu, L.; Gan, Y.; Kadambot, H.M.S. Gobi agriculture: An innovative farming system that increases energy and water use efficiencies. A review. *Agron. Sustain. Dev.* **2018**, *38*, 62. [CrossRef]
7. Paradiso, R.; Proietti, S. Light-quality manipulation to control plant growth and photomorphogenesis in greenhouse horticulture: The state of the art and the opportunities of modern LED systems. *J. Plant Growth Regul.* **2022**, *41*, 742–780. [CrossRef]
8. Liu, F.; Zhang, Z.; Zhao, X.; Wang, X.; Zou, L.; Wen, Q.; Yi, L.; Xu, J.; Hu, S.; Liu, B. Chinese cropland losses due to urban expansion in the past four decades. *Sci. Total Environ.* **2019**, *650*, 847–857. [CrossRef]

9. Tong, G.; Chen, Q.; Xu, H. Passive solar energy utilization: A review of envelope material selection for Chinese solar greenhouses. *Sustain. Energy Techn.* **2022**, *50*, 101833. [CrossRef]
10. Liu, X.; Li, H.; Li, Y.; Yue, X.; Tian, S.; Li, T. Effect of internal surface structure of the north wall on Chinese solar greenhouse thermal microclimate based on computational fluid dynamics. *PLoS ONE* **2020**, *15*, e0231316. [CrossRef]
11. Chen, C.; Yu, N.; Yang, F.; Mahkamov, K.; Han, F.; Li, Y.; Ling, H. Theoretical and experimental study on selection of physical dimensions of passive solar greenhouse for enhance energy performance. *Sol. Energy* **2019**, *191*, 46–56. [CrossRef]
12. Wu, X.; Liu, X.; Yue, X.; Xu, H.; Li, T.; Li, Y. Effect of the ridge position ratio on the themal environment of the Chinese solar greenhouse. *Roy. Soc. Open Sci.* **2021**, *8*, 201707. [CrossRef]
13. Zhang, Y.; Zhao, S.; Cheng, J.; Wang, P.; Lu, N.; Ma, C.; Xing, W.; Zheng, K. An Air Convection Wall with a Hollow Structure in Chinese Solar Greenhouses: Thermal Performance and Effects on Microclimate. *Agronomy* **2022**, *12*, 520. [CrossRef]
14. Mobtaker, H.G.; Ajabshirchi, Y.; Ranjbar, S.F.; Matloobi, M. Simulation of thermal performance of solar greenhouse in northwest of Iran: An experimental validation. *Renew. Energy* **2019**, *135*, 88–97. [CrossRef]
15. Zhang, X.; Lv, J.; Dawuda, M.M.; Xie, J.; Yu, j.; Gan, Y.; Zhang, J.; Tang, Z.; Li, J. Innovative passive heat-storage walls improve thermal performance and energy efficiency in Chinese solar greenhouses for non-arable lands. *Sol. Energy* **2019**, *190*, 561–575. [CrossRef]
16. Ali, S.; Deshmukh, S.P. An overview: Applications of thermal energy storage using phase change materials. *Mater. Today* **2020**, *26*, 1231–1237. [CrossRef]
17. Esmaeli, H.; Roshandel, R. Optimal design for solar greenhouses based on climate conditions. *Renew. Energy* **2020**, *145*, 1255–1265. [CrossRef]
18. Taki, M.; Rohani, A.; Rahmati-Joneidabad, M. Solar thermal simulation and applications in greenhouse. *Inf. Process. Agric.* **2018**, *5*, 83–113. [CrossRef]
19. Dong, X.; Huang, S.; Yu, L.; Li, S. Microclimate Environment Test for Wide-span Plastic Greenhouse with External Thermal Insulation. *Chin. J. Agrometeorol.* **2020**, *41*, 413.
20. Gorjian, S.; Ebadi, H.; Najafi, G.; Chandel, S.; Yildizhan, H. Recent advances in net-zero energy greenhouses and adapted thermal energy storage systems. *Sustain. Energy Techn.* **2021**, *43*, 100940. [CrossRef]
21. Wang, S.; Zhang, G.; Liu, X.; Wu, K.; Liu, F.; Wei, M. Heat and moisture transfer and heat storage and release performance of assembled soil sandwich wall in solar greenhouse. *Trans. Chin. Soc. Agric. Eng. Commun.* **2019**, *35*, 209–217.
22. Zhou, C.D. Zhou investigated a kind of assembled solar greenhouse with spray cotton light insulation material as wall and back roof. *Agric. Eng. Technol.* **2018**, *38*, 44–52.
23. Li, Y.; Yue, X.; Zhao, L.; Xu, H.; Liu, X.; Li, T. Effect of north wall internal surface structure on heat storage-release performance and thermal environment of Chinese solar greenhouse. *J. Build. Phys.* **2022**, *45*, 507–527. [CrossRef]
24. Zhu, F.; Zhou, Y.; Zhu, S. Experimental study on heat transfer in soil during heat storage and release processes. *Heat. Mass. Transfer.* **2021**, *57*, 1485–1497. [CrossRef]
25. Yadav, A.A.; Yadav, A.V.; Bagi, J.S.; Prabhu, P.A. Design of a Solar Modified Greenhouse Prototype. *J. Sci. Technol.* **2021**, *6*, 118–125.
26. Vitoshkin, H.; Barak, M.; Shenderey, C.; Haslavsky, V.; Arbel, A. Improving greenhouse insulation through multilayer thermal screens using the hot box method. In Proceedings of the 5th World Congress on Mechanical, Chemical and Material Engineering (MCM19), Lisbon, Portugal, 15–17 August 2019; pp. 15–17.
27. Zhao, P.; Song, M. Test and analysis of the modular cotton-polyester wall solar greenhouse thermal performance. *J. Chin. Agric. Mech.* **2018**, *39*, 44–47+70.